Evidence of a dual mechanism of action underlying the anti-proliferative and cytotoxic effects of ammonium-alkyloxy-stilbene-based α7- and α9- nicotinic ligands on glioblastoma cells.

Susanna Pucci[1,2], Cristiano Bolchi[3], Francesco Bavo[3], Marco Pallavicini[3], Clara De Palma[4], Massimiliano Renzi[5], Sergio Fucile[5,6], Roberta Benfante[1,2,4], Simona Di Lascio[4], Donatella Lattuada[4], Jean-Louis Bessereau[7], Manuela D'Alessandro[7], Valerie Risson[7] Michele Zoli[8], Francesco Clementi[1,2,4], and Cecilia Gotti[1,2,4]

Running title

Cytotoxic compounds against glioblastoma cells

[1]CNR, Institute of Neuroscience, Milan, Italy,
[2]NeuroMi Milan Center for Neuroscience University of Milano Bicocca,Italy.
[3]Dipartimento di Scienze Farmaceutiche, Università degli Studi di Milano, 20129 Milano, Italy
[4]Department of Medical Biotechnology and Translational Medicine, Università degli Studi di Milano,20129 Milan, Italy
[5]Dipartimento di Fisiologia e Farmacologia, Sapienza Università di Roma, 00185 Roma, Italy
[6]I.R.C.C.S. Neuromed, Via Atinese 18, 86077 Pozzilli, Italy
[7] Univ Lyon, Université Claude Bernard Lyon 1, CNRS UMR 5310, INSERM U 1217, Institut NeuroMyoGène, Lyon, France.
[8]Department of Biomedical, Metabolic and Neural Sciences, Center for Neuroscience and Neurotechnology (CfNN), University of Modena and Reggio Emilia, 41125 Modena, Italy

Corresponding author:
Dr. Cecilia Gotti,
CNR, Institute of Neuroscience
c/o Università di Milano-Bicocca
Edificio U28, Via Follereau 3,
20854 Vedano al Lambro(MB)
Email: cecila.gotti@in.cnr.it

Abstract

Glioblastomas (GBMs), the most frequent brain tumours, are highly invasive and their prognosis is still poor despite the use of combination treatment.

MG624 is a 4-oxystilbene derivative that is active on α7- and α9-containing neuronal nicotinic acetylcholine receptor (nAChR) subtypes. Hybridisation of MG624 with a non-nicotinic resveratrol-derived pro-oxidant mitocan has led to two novel compounds (StN-4 and StN-8) that are more potent than MG624 in reducing the viability of GBM cells, but less potent in reducing the viability of mouse astrocytes.

Functional analysis of their activity on α7 receptors showed that StN-4 is a silent agonist, whereas StN-8 is a full antagonist, and neither alters intracellular [Ca^{2+}] levels when acutely applied to U87MG cells. After 72 hours of exposure, both compounds decreased U87MG cell proliferation, and pAKT and oxphos ATP levels, but only StN-4 led to a significant accumulation of cells in phase G_1/G_0 and increased apoptosis. One hour of exposure to either compound also decreased the mitochondrial and cytoplasmic ATP production of U87MG cells, and this was not paralleled by any increase in the production of reactive oxygen species.

Knocking down the α9 subunit (which is expressed at relatively high levels in U87MG cells) decreased the potency of the effects of both compounds on cell viability, but cell proliferation, ATP production, pAKT levels were unaffected by the presence of the noncell-permeable α7/α9-selective antagonist αBungarotoxin. These last findings suggest that the anti-tumoral effects of StN-4 and StN-8 on GBM cells are not only due to their action on nAChRs, but also to other non-nicotinic mechanisms.

Key words: AKT1; apoptosis; ATP; cell cycle; glioblastoma cell lines; α7/α9 neuronal nicotinic receptors; proliferation; oxystilbene

1.Introduction

Glioblastomas (GBMs) are the most frequent and most aggressive malignant central nervous system (CNS) tumours arising from glial cells [1]. Their global incidence is <10 *per* 100,000 people and has increased over the last decade [2], median patient survival is approximately 14-17 months [3], and the 5-year survival rate is only 5.1% [4]. The usual treatment of GBMs is surgical resection followed by radiotherapy and chemotherapy with temozolomide (TMZ) [5], but the development of resistance to TMZ leads to high rates of recurrence and mortality. It is now thought that stem-like cells within the CNS are the origin of various primary brain tumours, including GBMs [6, 7], and drive the recurrence of GBMs [8].

Although new approaches involving combinations of multiple inhibitors and the identification of key driver mutations specific to each patient have recently been proposed (reviewed in [5, 9]), the dismal prognosis of patients with GBM means that there is still a need to improve our understanding of GBM biology in order to develop more successful therapeutic strategies.

It has recently been shown that GBM tumours, GBM cell lines, and GBM cancer stem cell lines express acetylcholine receptors [10-13] In particular, our group has shown that neuronal nicotinic acetylcholine receptors (nAChRs) containing the α7 and/or α9/α10 subunits are present in GBM cells and, when activated by nicotine or choline, show pro-proliferative activity that is effectively blocked by α7- and/or α9-contaning subtype-specific receptor antagonists [13]. Pharmacological characterisation of these receptors has shown that they are similar to those expressed by the A549 adenocarcinoma cell line, whose nicotine-induced activation also increases cell proliferation [14]. However, this proliferation is prevented by the previously characterised 4-oxystilbene selective nicotinic ligand MG624 [15, 16], which blocks ACh-induced current in oocytes expressing the α7 and α9/α10 subtypes at very low nM concentrations [14, 17]. Relatively low MG624 concentrations also potently counteract the increased cell proliferation induced by nicotine, and decrease nicotine-induced activation of the p-ERK and p-AKT pathways [14]. Brown *et al*. [18] have shown that MG624 potently suppresses the proliferation of primary human microvascular endothelial cells of the lung (HMEC-Ls), has robust anti-angiogenic effects on Matrigel models, rat aortic ring, and rat retinal explant assays, and suppresses the pro-angiogenic activity of nicotine in human H69 small cell carcinoma tumors in vivo, in the chicken chorioallantoic membrane and nude mice models.

In addition to being a competitive α7 and α9-α10 ligand, the stilbene structure of MG624 makes it very similar to resveratrol which, among its other activities [19], has anti-proliferative and pro-apoptotic effects on various tumour-derived cells (reviewed in [20]). In 2008, Biasutto *et al*. [21] combined the structures of the polyphenol resveratrol and the triphenylphosphonium cation by means of a 4-carbon-long linker to obtain (4-triphenylphosphoniumbutyl)-4-O-resveratrol iodide, and Sassi *et al* [22], demonstrated that this compound and its methylated analogue RDM-4'BTPI (which has greater anti-tumoral activity) induced the necrotic death of fast-growing cancer cells.

As RDM-4'BTPI shares some of the structural features of MG624 (its onium head, alkyl linker, and stilbene scaffold), we tested the effects of both on A549 adenocarcinoma and U87MG malignant glioma cell lines and found that they had cytotoxic effects on both [17], although MG624 was more selective and less toxic on non-tumoral cells. Consequently, in order to create a new and more effective anti-GBM agent that retains specificity for the nAChRs known to be involved in cancer progression, we synthesised hybrid molecules and tested their binding affinity for the α7 subtype, their ability to block ACh-evoked currents in *Xenopus* oocytes expressing human α7 and α9/α10 receptors, their anti-proliferative effects on various tumour cells expressing α7 and/or

α9/α10 nAChRs, their effects on mitochondrial reactive oxygen species (ROS) production, and their capacity to impair ATP production [17].

The aim of this study was to elucidate the mechanisms of action of two ammonium-headed elongated derivatives of MG624 (StN-4, which has a four-carbon linker resembling that of RDM-4'BTPI, and StN-8, which has an eight-carbon linker) (see Fig 1) underlying their antiproliferative and cytotoxic effects on GBM cells and functionally characterise their effects on nAChRs.

2. Materials and methods

2.1 Materials

αBgtx (α-Bungarotoxin) was purchased from Tocris Bioscience (Biotechne).

2.2 Compound Synthesis and binding studies

MG624, StN-4 and StN-8 were synthesized from commercial 4-(*E*)-stilbenol as previously reported [15, 17], and their affinities for the α7 subtype were determined as previously reported [17].

2.3 Cell culture

The human U87MG and GBM5 GBM cells were kindly provided by Dr. Antonio Daga (IRCSS – San Martino Hospital, Genoa, Italy). The U87MG cells came from ATCC®, and TMZ-resistant GBM5 cells were selected from a cancer stem cell (CSC)-enriched culture of patient-derived GBM cells [23].

The U87MG cells were grown in a high glucose DMEM medium (Gibco®, Life Technologies) supplemented with 10% fetal bovine serum (Carlo Erba Reagents) of South American origin, 2 mM L-glutamine (100x 200 mM solution, Euroclone), 100 U/ml penicillin G, and 100 µg/ml streptomycin (100x solution, Euroclone).

The GBM5 cells were grown in a 1:1 solution of DMEM/F-12 (Gibco®, Life Technologies) and Neurobasal™ (Gibco®, Life Technologies), supplemented with 1% B-27™ Supplement minus vitamin A (50x solution, Gibco®, Life Technologies), 20 ng/mL human EGF (Gibco®, Life Technologies), 2 mM L-glutamine, 100 U/mL penicillin G, and 100 µg/mL streptomycin. The plastic surfaces were pre-treated with a 1:250 solution of Matrigel® Matrix GFR (Growth Factor Reduced, Corning) and DMEM/F-12 or Neurobasal™ for at least 30 min at 37°C in order to promote cell adesion.

The cells were maintained in a 5% CO_2 environment at 37°C and those used in the experiments were between passage 2 and 12.

Mouse astrocytes were cultured in a MEM medium with HEPES (Gibco, ThermoFisher Scientific), supplemented with 10% heat-inactivated fetal bovine serum of South American origin, 0.6% glucose, 1 mM sodium pyruvate (100x 100 mM solution, Gibco, Thermo Fisher Scientific), 2 mM L-glutamine, 100 U/ mL penicillin G, and 100 µg/ mL streptomycin. The plastic surfaces were overnight pre-treated with 0.02 mg/ mL poly-D-Lysine (Merck KGaA) solution in borate buffer 0.1 M pH 8.5 at room temperature before seeding the cells. Mouse astrocyte cultures were kindly provided by Michela Matteoli's group (Humanitas University, Milan, Italy) and the cells were only emlpoyed at passage 1 for the experiments.

2.4 Total RNA extraction and reverse transcription

Total RNAs were extracted using the *RNeasy Mini kit or Micro Kit* and accompanying *QIAshredder* (Qiagen), according to the manufacturer's instructions. Briefly, a maximum of 5 x 10^6 cells, or cells harvested from multiwell plates, were collected by centrifugation and lysed with 350 μL of buffer RLT, containing β-mercaptoethanol (10 μL/mL RLT buffer), respectively. The lysate was homogenized by means of QIAshredder column centrifugation for 2 min at maximum speed. To avoid DNA contamination, samples were on-column incubated with DNAse I for 15 min and RNA was eluted with 50 μL (*Mini Kit*) or 14 μL (*Micro Kit*) of RNase-free water. The amount of eluted total RNA was determined by spectrophotometer at 260 nm and its purity was evaluated using the 260/280 ratio. 0.5–1 μg per sample was reverse transcribed using the GoScriptTM Reverse Transcriptase (Promega), according to information provided by the company.

2.4.1 Quantitative real-time PCR (q-PCR)

Gene expression analyses were performed by qPCR assay using the ABI Prism Thermocycler QuantStudio 5. The target sequences were amplified from 50 ng of cDNA in the presence of TaqMan® Universal Master Mix II, no UNG (Life Technologies, Inc.). The TaqMan® primer and probe assays used were human *CHRNA7* (ID #Hs01063373_m1), *CHRFAM7A* (ID #Hs04189909_m1), *CHRNA9* (ID #Hs00214034_m1), *CHRNA10* (ID #Hs00220710_m1), *GAPDH* (ID #Hs99999905_m1) was used as endogenous control, as described in the figure legends. The expression level of each subunit in the U87MG and U87MG/α9 KO cell lines, was determined by four independent experiments, run in triplicate. The "Quant Studio DA2 software (Thermo Fisher)" was used to calculate the mean value of the four replicates, according to the $2^{-\Delta CT}$ method.

2.5 Cell viability assay

Cell viability was assessed using the CellTiter 96 AQueous One Solution Cell Proliferation Assay (Promega) which is based on the reduction of water-soluble MTS tetrazolium salt by viable cells. The resulting formazan dye was quantified at an absorbance at 490 nm using PerkinElmer Inc. Wallac 1420 VICTOR2™ microplate reader.

The cells were plated in 24-well plates at different densities for each cell line: 12-15 × 10^3 U87MG and GBM5 or 50 × 10^3 for the mouse astrocytes. Mouse astrocytes were rendered quiescent by reducing serum concentration of the growth medium from 10 to 2%; the lowest serum percentage was kept for the entire treatment period. Three separate wells for each condition, including untreated controls, were assured. All of the tumoural and control glial cells were incubated with increasing concentrations of the compounds for 72 hours starting the day after plating. Complete medium with desired compound was refreshed once a day. After 72 hours of compound exposure, the cells were washed with PBS, fresh medium was added, and 50 µl of the MTS solution was pipetted into each well and depending on the metabolic activity, the cells were incubated between 45 min to 4 h at 37°C.

The absorbance of the control cells (not treated with the compounds) in the MTS assays was assumed to be 100%. The drug-induced decrease in viability was calculated as a percentage of that of the untreated control cells. The IC_{50} values of each compound for each cell line were calculated by employing GraphPad Prism software, version 6.0 using inhibitory normalized concentration-response equations.

2.6 Proliferation assay

On the day before treatment with the designated chemical, 5-15 x 10^3 U87MG cells were seeded in 24-well multiwells.

The nicotinic antagonist αBgtx (1 μM) was pre-incubated 30 min at 37°C before adding MG624, StN-4 or StN-8 at the indicated concentrations. The treatments were 72 hours long with change of the antagonists and the compounds every 24 hours.

After 72 hours the cells were trypsinised, resuspended in 600 μL of phosphate-buffered saline (PBS), and counted manually for a total of three times using a Bürker chamber.

Each 24-well plate in the proliferation assays was equally randomised to one of four experimental conditions plated in duplicate, triplicate or sextuplicate (one basal, one treated with MG624, StN-4 or StN-8, one pre-treated with αBgtx and one of the three compounds above-mentioned and the fourth one treated with αBgtx alone).Three separate fields were counted for each well, and the independent values generated by each well under the same experimental condition were averaged. One plate represented a single experiment under each experimental condition, and the number of separate experiments is shown in the figure 4 (the number in the lower part of the bar). The independent values (n) generated by the separate experiments (including outliers) were used for the statistical analysis.

2.7 *ATP production assay*

ATP concentrations were determined using a luciferin-luciferase method. After one-hour or 72 hours exposure with the desired compounds, 10^6 cells/treatment were resuspended in buffer-A (150 mM KCl, 25 mM Tris-HCl, 2 mM EDTA, 0.1% BSA, 10 mM potassium phosphate, and 0.1 mM $MgCl_2$, pH 7.4) and incubated for 1 min with digitonin (10 μg/10^6 cells) at room temperature by gently shaking. αBgtx was pre-incubated 30 min before adding MG624, StN-4 or StN-8. In the case of 72 hours treatment, fresh medium with compounds (and αBgtx where needed) was replaced once a day. The cells were distributed and plated in white 96-well multiwells at a density of 1-2 × 10^5 cells/well. The samples were treated with a mix containing 2 mM malate, 1 mM pyruvate, 1 mM ADP, and buffer-B containing 0.2 mM luciferin (D-luciferin, Merck KGaA) and 5 μg/mL luciferase (luciferase from *Photinus pyralis*/firefly, Merck KGaA) in 0.5 M Tris-acetate (pH 7.75). 2 μg/mL oligomycin (oligomycin A, Merck KGaA) was also added to detect glycolytic ATP that was measured using a GloMax® Discovery luminometer (Promega).

The concentration of ATP produced by oxidative phosphorylation was obtained by subtracting the glycolytic ATP amount from the total ATP concentration.

2.8 *Total intracellular ROS detection*

U87MG cells were seeded in 6-well plates at a density of 4 × 10^5 cells/well and, on the following day, they were deprived of serum. The day after, the cells were incubated for 45 min with 20 μM 2',7'-dichlorodihydrofluorescein diacetate (H_2DCFDA, Invitrogen Corporation, Thermo Fisher Scientific) in a medium without serum and phenol red. The dye was then washed out and the cells incubated with the desired compounds for 4 hours. After incubation the cells were trypsinised, washed and resuspended with 500 μL of HBSS supplemented with calcium and magnesium. In each experiment we employed U87MG cells treated with 50 μM *tert*-Butyl hydroperoxide solution, (TBHP, Merck KGaA) as a positive control.

The fluorescence signal was assessed using BD FACSCAlibur flow cytometer. Data analysis was performed by employing the BD CellQuest Pro software.

2.9 *Apoptosis assay*

U87MG cells were seeded in 6-well multiwells the day before treatment at a density of 2-3 x 10^5 cells/well. The samples were then incubated with the designated compounds for 72 hours in a medium without phenol red. Fresh compounds at the desired concentrations were then added back once a day. After 72 hours, the supernatants were collected, the cells were detached from plastic, washed and resuspended with 200 µL of Annexin V binding buffer provided with the kit (Dead Cell Apoptosis Kit with Annexin V-FITC and propidium iodide (PI) for flow cytometry, Invitrogen Corporation, ThermoFisher Scientific). Annexin V and PI were added to the samples and incubated for 30 min at room temperature by keeping the tubes in the dark. 300 µL of Annexin V binding buffer were then added to each tube and the fluorescence signals assessed.
The fluorescence signals were detected using BD FACSCAlibur flow cytometer. Data analysis was performed by employing the BD CellQuest Pro software. The resulting apoptotic rate was calculated by adding up the Annexin V-positive cells (early apoptotic) with the double positive Annexin V + PI-positive cells (late apoptotic).

2.10 *Cell cycle analysis*

U87MG cells were seeded in 6-well multiwells the day before treatment at a density of 2-3 x 10^5 cells/well. The samples were then incubated with the designated compounds for 72 hours in complete medium, which was refreshed once a day. After 72 hours, the cells were detached from plastic, washed and fixed in cold 70% ethanol for at least 2 hours at 4°C. The samples were then washed in PBS and stained with 10 µg PI (Invitrogen Corporation, Thermo Fisher Scientific) and 5 µg RNase A (Thermo Fisher Scientific) to remove RNA traces.
The fluorescence signals were detected using BD FACSCAlibur flow cytometer. Data analysis was performed by employing the BD CellQuest Pro software.

2.11 *CRISPR/Cas9 genome editing of U87MG cells*

A total of 200 µM crRNA and 200 µM tracrRNA (purchased from Integrated DNA Technologies/IDT, Inc.) were combined to form a duplex (gRNA) by running an annealing protocol on a Bio-Rad Thermal Cycler (Bio-Rad). After the annealing, gRNA was combined with 62 µM Cas9 nuclease (Integrated DNA Technologies/IDT, Inc.) and the mix incubated at room temperature for 15-20 min to form ribonucleoprotein (RNP) complex.
Two different crRNAs - and therefore two different RNPs - were chosen by analysing *CHRNA9* gene sequence with Benchling platform support, in order to ensure a successful RNA-guided Cas9 DNA cleavage.

10^6 U87MG cells were detached from plastic, washed and resuspended in 100 µL of electrolytic buffer (125 mM NaCl, 5 mM KCl, 1.5 mM $MgCl_2$, 10 mM glucose, 20 mM HEPES pH 7.4). RNPs were placed in an empty tube and the previously prepared suspension of cells added. The solution was then moved to a 4 mm gap cuvette (BTX Electroporation Cuvette Plus, BTX) by avoiding bubbles and subjected to electroporation through a BTX electroporator (BTX) by using a single 5-msec pulse of 300 V. 500 µL of pre-warmed complete medium was quickly added to the electroporated suspension and the cells were transferred to a 6-well plate already supplied with complete pre-warmed culture medium. After 24 hours, the medium was changed. After 48 hours from electroporation, the bulk cells were trypsinised, counted and seeded in a 96-well plate by following the limiting dilution method with serial 1:10 dilutions of cell suspension, eventually plating 1 cell/well.

Complete medium was changed every 2-3 days and the cell growth assessed by means of an inverted microscope. Before reaching confluency, pure clonal populations were trypsinised, split, frozen or subcultured and screened for *CHRNA9* deletion through PCR.

Genomic DNA extraction was performed by using QuickExtract™ DNA Extraction Solution (Lucigen Corporation) and following the manufacturer's instructions by using a Bio-Rad Thermal Cycler (Bio-Rad), where also PCR amplifications were run.

PCR amplification products were then loaded onto 1% agarose gels and stained with SYBR™ Safe DNA Gel Stain (Invitrogen Corporation, Thermo Fisher Scientific) for visual evaluation through a transilluminator.

PCR reactions were initially run to verify the correct RNA-guided Cas9 DNA cleavage in bulk cells and then to assess the presence of pure populations after limiting dilution cloning, by employing several suitable primer pairs (Integrated DNA Technologies/IDT, Inc.).

2.12 AKT1 pathway activation detection through *Western blotting and signal intensity quantification of bands*

The day before treatment, 7-9 x 10^4 U87MG cells were seeded in 24-well multiwells.

The cells were then treated with the indicated concentrations of MG624, StN-4 or StN-8, in the presence or absence of 1 μM αBgtx (which was pre-incubated or not for 30 min at 37°C) for 72 hours. In each multiwell there were always one or two control wells with cells that did not receive any compound and one or two wells that received 1 μM αBgtx alone. The treatments were 72 hours long with change of the antagonists and/or the compounds every 24 hours.

After the incubation, 80-90 µL of Laemmi sample buffer were added to each well, the cells were scraped and lysed and subjected to SDS-PAGE. Samples were separated by means of SDS-polyacrylamide gel electrophoresis using 9% acrylamide, and electrophoretically transferred to nitrocellulose membranes with 0.45 µm pores (GE Healthcare Amersham).

The blots were blocked overnight in Tris-buffered saline (TBS) 4% non-fat milk (Hipp 2), washed in a buffer containing TBS 4% non-fat milk and 0.3% Tween 20® (Merck), incubated for 2 hours at room temperature with the primary antibodies and then with the appropriate secondary antibodies for 1 hour at room temperature keeping the blots in the dark.

The primary antibodies were purchased from BD Transduction Laboratories (anti-human AKT1 mouse IgG1, ID #610860) and Invitrogen (anti-human pSer473-AKT1 rabbit IgG, Thermo Fisher Scientific ID #44-621G) used in accordance with the manufacturer's instructions.The secondary antibodies employed were from Li-Cor: goat anti-rabbit IRDye800RD ID #926-3221 and goat anti-mouse IRDye680RD ID #926-68070.

After ten washes with TBS with decreasing concentrations of Tween® 20 (starting from 0.3% to 0%), the membranes were dried overnight in the dark at room temperature. The immunoreactive signal was measured using an Odissey CLx Near-Infrared Imaging System (Li-Cor) and quantified through Image Studio software version 2.1.10.

After quantifying band intensity (expressed as pAKT/AKT ratio), the basal values or the mean values of the two wells under basal condition were considered as 1 and used to normalise the values of each blot under each condition. The experimental value for each plate under each experimental condition is the mean of the quantification of two gels loaded with samples from the same well treated in the same way and normalised to the basal value (or the mean of two basal values) within the corresponding blot. The numbers reported in the

figures are referred to independent experiments performed using independent plates.

2.13 *Electrophysiological experiments*

Electrophysiological assays used to outline the pharmacological profiles of MG624, StN-4 and StN-8 were performed by using GH4C1 cells stably expressing human α7-nAChR.

Whole-cell current recordings were performed 2-3 days after plating α7-nAChR-expressing GH4C1 cells. Recordings and data analysis were carried out using borosilicate glass patch pipettes (from 3 to 6 MΩ tip resistance) connected to an Axopatch™ 200 A amplifier (Axon Accessories, Molecular Devices). Data were stored on a computer using the Axon™ pCLAMP™ 10 software (Molecular Devices). During the recording period, cells were bathed in the following solution: 140 mM NaCl, 2 mM $CaCl_2$, 2.8 mM KCl, 2 mM $MgCl_2$, 10 mM HEPES/NaOH, and 10 mM glucose, pH 7.3. The patch pipettes were filled with a solution containing: 140 mM CsCl, 2 mM MgATP, 10 mM HEPES/CsOH, and 5 mM BAPTA, pH 7.3. Whole-cell capacitance and patch series resistance (5-15 MΩ) were estimated from slow transient compensations. A series resistance compensation of 85-90% was obtained in all cases. The cells were voltage-clamped at a holding potential of -70 mV and continuously perfused with a gravity-driven system using independent external tubes for the control and compound-containing solutions. These tubes were positioned 50-100 μm from the patched cell and connected to a fast exchanger system (RSC-160, BioLogic). Concentration-response relationships were constructed by sequentially applying different concentrations of MG624, StN-4 or StN-8 and normalizing the resulting current amplitudes to the value obtained by applying 200 μM ACh or 100 μM ACh plus 10 μM α7-selective PAM PNU120596. For quantitative estimations of MG624, StN-4 and StN-8 actions, concentration-response relationships were fitted to the following equation: $I = I_{max} \{[C]^{nH} / (EC_{50}{}^{nH} + [C]^{nH})\}$, where I is the current amplitude induced by the agonist at concentration [C], I_{max} denotes the maximal response of the cell, nH is the Hill coefficient, and half maximal excitatory concentration (EC_{50}) is the concentration for which a half maximum response is induced.

2.14 *Ca^{2+} mobilization*

Changes in free intracellular Ca^{2+} concentration ($[Ca^{2+}]_i$) were measured by time-resolved digital fluorescence microscopy, using an integrated acquisition system, composed of an upright reflected fluorescence microscope (Leica LMSA) and the Metafluor software (Molecular Devices). U87MG cells were incubated with the Ca^{2+} indicator Fura-2 acetoxylmethylester (1 μM) for 45 min at 37 °C in culture medium. The changes of $[Ca^{2+}]_i$ were expressed as $R = F_{340}/F_{380}$, where F_{340} and F_{380} are the fluorescence intensities measured from individual cells at an emission wavelength of 510 nm illuminating the specimen with 340 and 380 nm excitation wavelengths, respectively. Cells were continuously perfused during the experiment. The acquisition frequency was 0.33 Hz. Ca^{2+} mobilization was quantified by calculating the time integral of the Ca^{2+} signal during the application of agonists and normalising it to the time integral calculated for the same duration before the agonist application. This approach was used to minimize the noise due to the presence of spontaneous Ca^{2+} transients.

2.15 *Statistical analyses*

The number of experiments that were performed for each assay has been reported in the figures. Each sample in each experiment was at least duplicated. The qPCR experiments were performed four times for each cell line, and each sample was triplicated. The results are expressed as mean values ± SEM.

The MTS viability experiments were performed from five to nine times for each compound in each cell line. The parametric data were analysed using one-way ANOVA and, if there was a significance between-group difference, Bonferroni's *post hoc* test. The non-parametric data were analysed using a Kruskall-Wallis test followed by Dunn's *post hoc* test. The accepted level of significance was $p < 0.05$. All of the statistical analyses were made using GraphPad Prism software, version 6.0.

3.Results

3.1 *Pharmacological and functional characterisation of StN-4 and StN-8 on α7 and α9/α10 nicotinic receptors*

We have previously shown [17] that MG624, StN-4 and StN-8, whose chemical structures are shown in Figure 1, bind with high affinity to α7 receptors and compete with similar affinity to the ^{125}I-αBgtx binding to α7 receptors. Moreover, when tested on oocytes expressing the human α7 and α9/α10 subtypes, all three compounds block ACh-induced current with an IC_{50} (half maximal inhibitory concentration) in the nM range: the effect of StN-4 was similarly potent on both subtypes, whereas that of StN-8 was 10 times more potent on the α9/α10 subtype than on the α7 subtype [17].

When MG624 was first electrophysiologically characterised using the chick α7-nAChR subtype [16], it was described as a potent antagonist. However, recent studies have highlighted the existence of a new class of nAChR ligands (silent agonists) that have been described as very weak partial agonists but very effective desensitisers that induce relatively little or no channel activation, and readily drive nAChRs towards a non-conducting state that modulates signal transduction in non-neuronal cells [24]. We therefore carried out whole-cell patch clamp and two-electrode voltage clamp studies to test the effects of increasing concentrations of MG624, StN-4 and StN-8 on human α7-nAChRs stably expressed in GH4C1 cells in the absence and presence of the positive allosteric modulator (PAM) PNU120596. This assay is possible because the tested compounds orthosterically bind nAChRs, while the PAM binds allosteric sites. Figure 2A shows that increasing concentrations of StN-4 and StN-8 did not increase the current recorded from the cells overexpressing α7-nAChRs, whereas MG624 started to increase it at a concentration of 1 μM and, at 100 μM, averaged 40% of the response of 200 μM ACh. Moreover, in order to check whether the compounds behave as silent agonists and generate currents, they were tested at the low concentration of 100 nM in the presence of 10 μM of PNU120596 (Fig. 2B). Figure 2A shows that neither StN4 nor StN8, induced any current alone and, in the presence of PNU120596 (Fig. 2B), only the current induced by StN4 was increased, whereas the PAM failed to elicit any response when co-applied with StN-8. On the basis of this functional characterisation, it can be said that StN-4 is a silent agonist, StN-8 an antagonist, and MG624 a strong desensitiser at low (nM) concentrations and a partial agonist at high (μM) concentrations.

We also measured the Ca^{2+} mobilisation induced by the three compounds at concentrations corresponding to their IC_{50} values in viability assays (see below). As expected given its partial agonism, only MG624 significantly increased [Ca^{2+}] (Fig. 2C) whereas, acutely applied StN-4 and StN-8 did not alter [Ca^{2+}], which is in line with their respective pharmacological nature as a silent agonist and antagonist (Fig.2C).

3.2 *StN-4 and StN-8 decrease the viability of GBM cells*

The effect of MG624, StN-4 and StN-8 on the viability of U87MG and GBM5 cells was investigated using the MTS assay (Fig.3A) after 72 hours of treatment and, in order to compare the sensitivity of GBM cells to StN-4 and StN-8 with their sensitivity to MG624, GraphPad Prism 6 software was used to calculate their IC_{50} values (see table in Fig. 3B).

All three compounds decreased the viability of U87MG cells in a concentration-dependent manner: StN-4 (IC_{50} 1.5 μM) was more potent than MG624, but less potent than StN-8 (IC_{50} 100 nM); when tested on the GBM5 cell line (a culture enriched in GBM cancer stem cells) [23], the IC_{50} values of StN-4 and StN-8 were respectively 1.9 μM and 210 nM, that are very similar to those determined using U87MG cells (see table in Fig. 3B).

In parallel, the compounds were also tested on primary mouse astrocytes (a non-transformed model of glial cells) in order to evaluate their selectivity for cancer cells, especially GBM cells arising from the malignant transformation of glial cells. All three compounds reduced the viability of normal mouse astrocytes at concentrations that were 12-15 times higher than those required for human U87MG cells; similarly, they were 7-9 times more potent on GBM5 cells than on mouse astrocytes (see table in Fig. 3B).

3.2.1 *StN-4 and StN-8 are much less potent on α9-knockout U87MG cells*

As GBM cells express relatively high levels of α9 subunit mRNA [13], we investigated whether the deletion of this subunit affects the response of U87MG cells to the compounds by removing the *CHRNA9* gene encoding α9 subunit protein from the U87MG cell line using CRISPR/Cas9 technology. Figure 3C shows the results of an RT-PCR analysis of the editing of U87MG cell genome: the complete absence of α9 mRNA. Although the absence of α9 mRNA induced a slight increase in the expression of the α10 subunit, there was no change in the mRNA levels of *CHRNA7* (encoding the α7 subunit) or *CHRFAM7A* (encoding α7dup protein).

MG624 was 6-fold more potent on wild-type U87MG cells than on α9-knockout U87MG cells, whereas StN-4 and StN-8 were respectively 15- and 30-fold more potent on wild-type cells (Tab. 3B). These findings suggest that α9-containing receptors are important targets of our compounds for reducing the viability of GBM cells. This is particularly intriguing as it is known know that α7-nAChRs are highly expressed in the brain [25], whereas α9-containing subtypes are not [26].

3.3 *Non-nicotinic mechanisms involved in the anti-proliferative effects of StN-4 and StN-8 on GBM cells*

3.3.1 *The anti-proliferative effects of StN-4 and StN-8 on GBM cells are also due to non-nicotinic activity.*

We have previously shown that the incubation of U87MG cells with 1 μM αBgtx for 72 hours does not change basal cell proliferation [13]. As MG624, StN-4 and StN-8 competitively bind α7- and α9-containing nAChRs, we analysed whether they affect U87MG cell proliferation and whether this effect is altered by co-incubation with 1 μM αBgtx. To this end, we pre-incubated U87MG cells with saturating concentrations of αBgtx (1 μM) to block all surface α7- and α9-containing nAChRs, and then treated the cells for 72 hours with 4 μM MG624, 0.5 μM StN-4, or 0.25 μM StN-8, all concentrations within the range of the IC_{50} values determined by the viability assay.

As shown in Figure 4, all three treatments markedly reduced U87MG cell proliferation. Treatment with αBgtx alone for 72 hours did not affect basal cell proliferation, and its co-incubation with the compounds did not affect

the decrease in proliferation induced by the compounds themselves. This suggests that the anti-proliferative effects of these concentrations of the compounds are mainly due to non-nicotinic mechanisms.

3.3.2 *StN-4 and StN-8 decrease the ATP produced by oxidative phosphorylation and glycolysis in U87MG cells*

Mitochondria are central organelles of cell survival and death, and a decrease in mitochondrial membrane potential and ATP levels are critical signs of the latter. As targeting mitochondrial metabolism as a means of inducing the apoptosis of cancer cells is emerging as a successful treatment strategy, we analysed the effects of the three compounds on the ATP produced by the oxidative phosphorylation (OxPhos) and glycolysis of GBM cells. As we have previously reported that, after the incubation of U87MG cells with MG624, StN-4 and StN-8 for 72 hours at the IC_{50} concentrations previously determined by cell viability assays, there is a reduction of OxPhos ATP (Fig. 5A) [21], we analysed the effects of the compounds after shorter acute incubation for one hour and found that StN-4 and StN-8 significantly reduced the level of ATP produced by oxidative phosphorylation (Fig. 5B) and glycolysis (Fig. 5C), whereas MG624 did not significantly affect the overall production of OxPhos or glycolytic ATP under the same experimental conditions.

At the same time, we analysed the effect of 72 hours of MG624 treatment, and one and 72 hours of StN-4 and StN-8 treatment on U87MG cell ATP production in the presence of the non-cell permeable α7/α9-nAChR antagonist αBgtx in order to investigate whether the reduction in OxPhos and glycolytic ATP production induced by the compounds was mediated by their binding to the surface α7/α9-nAChRs on GBM cells. The results showed that pre-incubation with a saturating concentration of αBgtx did not reduce the effect of MG624, StN-4 and StN-8 on OxPhos ATP production after 72 hours (Fig. 5A) or the effect of StN-4 and StN-8 after one hour (Fig. 5B); it also had no effect on the production of glycolytic ATP (Fig.5C).

Cellular mitochondrial dysfunction can be reflected by the loss of the mitochondrial membrane potential, and we found that one hour of incubation with the compounds did not alter mitochondrial health, whereas 72-hour treatment greatly reduced mitochondrial potential as revealed by tetramethylrhodamine, methyl ester (TMRM) staining.

It can therefore be concluded that the effects of MG624, StN-4, and StN-8 on mitochondrial and cytoplasmic ATP production after one or 72 hours of incubation is not mediated interactions with cell membrane receptors, but probably occur through still unknown intracellular pathways favoured by their membrane permeability.

3.3.3 *StN-4 and StN-8 do not affect ROS production of U87MG cells*

Given their sudden effects on both mitochondrial and cytosolic ATP production, we also determined the possible effects of MG624, StN-4 and StN-8 on the production of ROS in U87MG cells.

We have previously found that neither StN-4 nor StN-8 has any effect on mitochondrial O_2^- production after acute incubation with increasing concentrations of the compounds, including those that decrease ATP levels in U87MG cells [21]. In the present study, we used H_2DCFDA staining followed by FACS analysis to measure the possible increase in cytoplasmic ROS in U87MG cells after four hours of treatment, with the potent oxidising agent tert-butyl hydroperoxide (TBHP) being used as a positive control. We did not observe any variation in total cellular ROS levels at compound concentrations capable of decreasing OxPhos and glycolytic ATP levels in the same cells after one hour of incubation (Fig.S1).

3.3.*4 StN-4 affects the U87MG cell cycle*

Given that the compounds significantly reduce GBM cell proliferation (see Fig.4), in order to investigate whether they alter the different phases of the cell cycle, we stained U87MG cells with propidium iodide to detect their DNA content through FACS analysis after 72 hours' treatment with MG624 4 μM, StN-4 2 μM or StN-8 0.25 μM. As shown in Figures 6A and 6B, in comparison with untreated controls, the cells treated with MG624 or StN-4 significantly accumulated in the G_1/G_o phase of the cell cycle, and there was a significant decrease in the fraction of cells in the S and G_2/M phases, whereas there was no difference between the cells incubated with StN-8 and the untreated cells.

This indicates that treatment with MG624 or StN-4 reduces the entry of GBM cells into the S phase of the cell cycle, and thus has a cytostatic effect.

3.3.5 *StN-4 induces apoptosis in U87MG cells*

Apoptosis is a major cause of cancer cell growth inhibition. We have previously shown that, by acting through nicotinic receptors containing α7 and/or α9/α10 subunits, nicotine stimulates the proliferation of U87MG and GBM5 cells and increases the phosphorylation of AKT kinase in Ser473 [13], whose signalling pathway activation prevents the apoptotic death of cancer cells.

In order to determine whether the anti-proliferative effect of MG624, StN-4 and StN-8 is due to increased apoptotic cell death, we used FACS analysis to measure the apoptotic rate (both early and late apoptosis) of U87MG cells treated for 72 hours with compound concentrations corresponding to the IC_{50} values determined by vitality assays. As shown in Figure 7, MG624 4 μM and StN-4 2 μM clearly showed pro-apoptotic activity; StN-8 0.25 μM also led to a slight induction of apoptosis but this was not statistically significant.

3.3.6 *StN-4 and StN-8 reduce basal activation of the AKT signalling pathway*

We have previously shown that nicotine and choline increase AKT phosphorylation in GBM cells, and that this activation may promote GBM cell proliferation [13]. As MG624, StN-4 and StN-8 block cell proliferation and are cytotoxic, we investigated whether they act by decreasing AKT pathway activation by treating U87MG cells with different compound concentrations for 72 hours and analysing the results by means of immunoblotting.

As shown in Figure 8, Western blotting revealed that all three compounds dose-dependently reduced AKT activation (tested by means of the specific detection of Ser473-phosphorylated AKT levels) and led to a decreased pAKT/total AKT ratio (Fig. 8A). In order to investigate whether this effect was due to the direct binding of the compounds to receptors on the plasma membrane of U87MG cells, this study was also carried out in the presence of the non cell-permeable α7/α9-nAChR antagonist αBgtx, and it was found that the decrease in the pAKT/AKT ratio induced by incubation of the cells with MG624, StN-4 or StN-8 was not affected by the presence of αBgtx during the 72 hours of treatment (Fig. 8B).

These findings are in line with the increased apoptosis and cell cycle blockade driven by MG624 and StN-4, and the reduced cell proliferation and viability induced by all three compounds.

4. Discussion

The findings of this study show that compounds StN-4 and StN-8, which are both analogues of MG624 (Fig. 1), and have a similar chemical structure, greatly inhibits the growth and survival of GBM cells. Both compounds act on α7 and α9/α10 nAChRs, and knocking down the α9 subunit in GBM cells decreases their potency. Both compounds also decrease mitochondrial and cytoplasmic levels of ATP and inhibit AKT phosphorylation, whereas only StN-4 leads to a significant accumulation of GBM cells in the G_1/G_0 phase of the cell cycle and increased apoptosis. Although MG624, StN-4 and StN-8 all interact with α7- and α9-containing nAChRs and through their interaction with α9 receptor greatly decrease GBM cell vitality, characterisation of their mechanisms of action in GBM cells showed that they also act through non-nicotinic mechanisms.

Our previous study [13] indicated that nAChRs are potential therapeutic targets for the treatment of GBM, which is why we evaluated the possible anti-GBM effects of new nicotinic compounds. It has been shown that natural compounds with a stilbene backbone have promising cancer prevention activity by targeting a wide variety of intracellular pathways (reviewed in [27, 28]), so we synthesised new compounds derived from the stilbene derivative MG624 that bind and block the α7 and α9-α10 subtypes with high affinity. Moreover, we and others have demonstrated that MG624 is cytotoxic for cancer cells *in vitro* [14, 29] and *in vivo* [18].

MG624 is a 4-oxystilbene derivative (see Fig. 1) with three different functional groups: the stylbenoxy residue at one end, the ammonium head at the other end, and the alkylene linker in between. We decided to keep the 4-oxystilbene scaffold of MG624 and optimise its oxyethylammonium portion, which is critical for receptor interaction. As the relative position of the oxygen and nitrogen atoms can be reasonably considered an important structural feature for the interaction, we first investigated the effect of elongating the chain linking the two heteroatoms, as was also suggested by results obtained using RDM-4'BTPI, a novel mitochondriotropic compound obtained by coupling resveratrol to the membrane-permeable lipophilic cation triphenylphosphonium. Given the structural similarity of MG624 and RDM-4'BTPI, we synthesised many new compounds by hybridising the two chemicals and, on the basis of their cytotoxicity for cancer cells expressing nAChRs, selected two elongated, ammonium-headed derivatives of MG624: one with a four-carbon linker resembling that of RDM-4'BTPI (StN-4), and the other with an eight-carbon linker (StN-8).

Functional analysis of their activity on α7 receptors showed that StN-4,is a silent agonist and StN-8 a full antagonist, which was also confirmed by their inability to increase intracellular $[Ca^{2+}]$ in GBM cells.

Unlike previous determinations of the potency in blocking ACh-induced current [17], the further functional characterisation performed in this study, indicates that α7 receptor activation is greatly affected by linker lengthening, which results in transition from partial agonism (MG624) to a silent agonism (StN-4), to antagonism (StN-8). This indicates that, in these analogues, altering inter-distance and reciprocal position of ammonium head and stilbene scaffold due to the lengthening of a flexible linker has a much larger impact on α7 receptor activation than on blockade of α7 response to ACh.

α9-, α9-α10- containing receptors are not normally expressed in mammalian brain [30] but we and others have previously reported [10-13] that GBM cells express nAChRs containing the α7 and /or α9 subunits, the most Ca^{2+} permeable nAChR subtypes [31, 32], and that stimulating these receptors with nicotine or choline increases the proliferation of GBM cells [10, 13]. These effects are due to interactions between the ligands and

surface α7- and/or α9-containing receptors because the presence of non cell-permeable peptide antagonists selective for α7- and/or α9-containing receptors blocks both ligand-induced and long-term basal proliferation. Moreover, silencing the expression of the α7 or α9 subunit by means of siRNAs, greatly and selectively reduces the effects of nicotine and choline on GBM cells**.**

We have previously shown that StN-4 and StN-8 are more active than MG624 on U87MG and in this paper demonstrated that they are also more active on GBM5 cells obtained from a cancer stem cell-enriched culture [22]. So we decided to investigate whether co-incubation with a classic competitive antagonist (αBgtx) affects their anti-proliferative effects by incubating U87MG cells with IC_{50} concentrations of the compounds, with or without saturating concentrations of αBgtx (Fig. 5). Under these experimental conditions, cell proliferation was not affected by αBgtx alone, but it was greatly decreased by StN-4 and StN-8, and pre- or co-incubation with αBgtx did not change these effects (Fig.5), thus indicating that the anti-proliferative outcome at IC_{50} concentrations determined by means of MTS viability assays is also due to non nAChR-mediated mechanisms. StN-4 and StN-8 are similarly active on A549 cells derived from lung tumours, which express both α7- and α9-containing nAChRs [14], and are more potent than MG624 (their potency is comparable to that observed in GBM cells). However, when tested on SH-SY5Y human tumour cells that express many nAChR subtypes but not those containing the α9 subunit, StN-4 and StN-8 had IC_{50} values that were 20-100 times higher than those found in GBM cells [21], which indirectly suggests that they act more strongly on α9-containing nAChRs than on α7-containing nAChRs. Both compounds are also less active in normal astrocytes than in GBM cells, thus indicating their preference for cancer cells.

In order to demonstrate the compounds' possibly greater effects on α9-containing receptors, we used CRISPR/Cas9 technology to create a novel α9-knockout U87MG cell line and found that both StN-4 and StN-8 had less potent effects on the α9-knockout cell line than on wild-type U87MG cells, thus confirming that α9-containing nAChRs are important targets for their anti-GBM activity. This finding, together with those of Thompson and Sontheimer [12] showing that *CHRNA9* expression is significantly higher In GBM samples than in non-tumoral samples and our previous data [13] showing that chronically blocking α9-containing receptors with subtype-specific toxins reduces the basal proliferation of U87MG cells, underlines the important role of α9- containing receptors in the basal proliferation of GBM cells. However, it must be said that, in comparison with the major role of other molecules involved in GBM proliferation [33, 34], the albeit significant involvement of nAChRs may not be biologically relevant.

A recent study by Thompson and Sontheimer [12] has shown the expression of nAChRs and muscarinic AChRs in GBM cell and patient-derived xenograft lines, the high expression of α9 mRNA, and the presence of all of the proteins necessary for acetylcholine synthesis and release, thus suggesting that GBM cells may use acetylcholine as an autocrine signalling molecule. Their calcium time-lapse studies have also shown that nicotine and an α7-specific compound activate Ca^{2+} influx in GBM cells over a very long time course of hundreds of seconds. As α7 receptors are rapidly desensitised [35], this long-lasting increase in intracellular Ca^{2+} may be due to the release of calcium from intracellular stores, as previously shown in hippocampal astrocytes [36]. Changes in Ca^{2+} are involved in various cell changes that are crucial for cancer progression, and so it is possible that blocking intracellular Ca^{2+} entry by means of StN-4 and StN-8 may affect responses involving multiple intracellular events.

The cytotoxic effects of MG64, StN-4 and StN-8 are not only related to their interactions with nAChRs, and we have now demonstrated that chronic treatment with StN-4 and StN-8 reduces GBM proliferation and p-AKT

phosphorylation. AKT is one of the most hyper-activated kinases in human cancers, and changes in AKT expression or activity may be an essential step in their onset or progression [29, 37]. AKT modulates cell proliferation, metabolism, survival, invasiveness and angiogenesis, and the over-expression of genes in the AKT pathway is also an important mechanism of drug resistance [38, 39]. Furthermore, the interruption of AKT phosphorylation leads to apoptosis, growth inhibition, and reduced invasiveness [40].

When added to cells for one hour at concentrations in the cytotoxic IC_{50} range, StN-4 and StN-8 both reduced the production of mitochondrial and glycolytic ATP and, when tested after chronic 72-hour incubation both reduced Ser473-AKT phosphorylation, but only StN-4 arrested the U87MG cell cycle by reducing entry into the S phase. An apoptosis/necrosis assay using annexin V-FITC/propidium iodide (PI) double staining showed that U87MG cells treated with StN-4 always had a very low percentage of necrosis, thus confirming that the presumptive mechanism of cell death attributable to StN-4 (and MG624) is apoptosis.

Mitochondria are organelles controlling ATP generation, redox homeostasis, metabolic signalling, and apoptotic pathways. Although glycolysis has been traditionally considered to be the major source of energy in cancer cells, it is now increasingly acknowledged that mitochondria play a key role in oncogenesis [41]. The effects of StN-4 and StN-8 on mitochondrial and glycolytic ATP are very important as it has been shown that cancer mitochondria switch between glycolysis and oxidative phosphorylation, and this seems to play a major role in multiple modes of resistance to oncogenic inhibition [41, 42]. Agents targeting both glycolysis and oxidative phosphorylation are therefore promising anti-cancer treatments. This is also very important because a small sub-set of treatment-resistant glioma stem cells (GSCs) are mainly responsible for malignant glioma regrowth and relapse. These cells have a higher level of total ATP than differentiated glioma cells, and GSCs obtained from a number of tested GBM cell lines tolerate the inhibition of glycolysis or oxidative phosphorylation very well, and only the combined inhibition of both leads to a substantial depletion of intracellular ATP [43].

We believe that the decrease in cytosolic and mitochondrial ATP is due to the previously demonstrated ability of StN-4 and StN-8 to permeate cell membranes [17]. Moreover, as they have an N head that is positively charged, they can concentrate inside mitochondria because their high negative transmembrane potential is higher in tumour cells. This mechanism may explain why the compounds are more selective of tumour cells than their non-tumoral counterparts.

Furthermore, several recent studies by the group of Marina Skok have reported that nAChRs containing the α7 or the α9 subunits are found on the mitochondrial outer membrane of different cells where they regulate the release of pro-apoptotic factors. [44-46]. As our compounds are cell permeable, that at least part of their anti-tumoral activity be mediated by an interaction with mitochondrial nAChRs is a distinct possibility that deserves additional investigations on isolated mitochondria.

In conclusion, our findings show that StN-4 and StN-8 have potent anti-tumoral activity against GBM cells. Some of their effects are mediated by interactions with α7- and/or α9-containing nAChRs, but others are nAChR-independent probably because the different number of methylene groups in the alkyl linker of their chemical structures affects their lipophilicity and allows them to interact differently with biomembranes.

Further studies are needed in order to discover whether these antiproliferative and cytotoxicity mechanisms are independent or have a cooperative or additive effect. Exploring these new pathways seems to be a promising means of developing a novel therapeutic approach to GBMs.

5. Funding

Dr Susanna Pucci is recipient of a fellowship from the Fondazione Vollaro, (Milano).
This work was supported by Fondazione Monzino (Milano) and from the Fondazione Vollaro (Milano).

6. Declaration of competing interest

All the other authors declare that do not have conflict of interest with no actual or potential conflict of interest including any financial, personal or other relationships with other people or organizations within three years of beginning the work submitted.

7. References

8. Figure legends

Figure 1: **Chemical structure of MG624, StN-4, StN-8.**

Figure 2: MG624, StN-4 and StN-8 have different pharmacological nicotinic profiles.
A) Whole-cell patch-clamp analysis of the effects of increasing concentrations of MG624, StN-4 or StN-8 on human α7 subtype-overexpressed in GH4C1 cells. The activation responses are normalised to the maximal response of 200 µM ACh. MG624 is a partial agonist of human α7 nAChR at concentrations higher than 1 μM.
B) Up, typical traces of whole-cell inward current elicited in human α7 subtype-overexpressing GH4C1 cells by ACh 100 μM, MG624 0.1 μM and StN-4 0.1 μM, in the presence of PAM PNU12059 10 μM. Bottom, whole-cell patch-clamp analysis of the effects of 0.1 μM of MG624, StN-4 or StN-8 co-applied with 10 µM of PNU120596 on human α7 subtype-overexpressed in GH4C1 cells. In this case the responses were normalised to those obtained by 100 µM ACh + 10 µM PNU120596. StN-4 is a silent agonist of human α7 nAChR.
C) Up, typical time-courses of $[Ca^{2+}]i$ changes elicited by MG624 application (4 µM, horizontal line) in two different U87MG cells. Bottom, bar graph showing the Ca^{2+} mobilization induced by the indicated molecules, normalised to the spontaneous Ca^{2+} mobilization observed in the same cells before the drug administrations (see methods). *, $p<0.001$.

Figure 3:
A) Viability assay curves of U87MG and GBM5 cells after 72 hours of exposure with the indicated concentrations of MG624, StN-4 and StN-8.
B) In the table are shown the IC_{50} values determined from MTS viability assay curves performed on the indicated cell types. The IC_{50} values (+/- 95% confidence interval CI) were calculated from concentration-response curves fitted by a nonlinear regression analysis.
C) RT-PCR analysis of nAChR gene expression in the wild-type U87MG cells (black bars) and in the □9-knockout U87MG cells (grey bars). The expression of nicotinic subunit mRNAs is normalised over GAPDH mRNA according to the $2^{-\square Ct}$ method (n =4).

Figure 4

Effect of the α7/α9 antagonist αBgtx on the antiproliferative effect of MG624, StN-4 and StN-8. U87MG cells proliferation is not decreased by 72-hour exposure to 1 μM αBgtx, but is strongly decreased by exposure to 4 μM MG624 or 0.5 μM StN-4 or 0.25 μM StN-8 and it is not affected by preincubation and co-incubation of the compounds with 1 μM αBgtx (left bar). **p < 0.01, ***p < 0.001, ****p < 0.0001: decrease of cells treated with the compounds over untreated cells. The data were analysed by means of a one-way ANOVA followed by a Bonferroni's post hoc test

Figure 5

MG624, StN-4 and StN-8 decrease ATP produced by oxidative phosphorylation (OXPHOS) or glycolysis. U87MG cells were exposed for 72 hours **(A)** or 1hour (B**)** to each compound at the indicated concentrations in the presence or absence of 1 μM αBgtx. Part **C** of the figure shows the quantification of the decrease of glycolytic ATP detected after 1 hour of exposure to the indicated concentration of the compounds. *p < 0.05, **p < 0.01, ***p < 0.001, ****p < 0.0001: decrease over untreated cells. The data were analysed by means of a one-way ANOVA followed by a Bonferroni's post hoc test.

Figure 6

Effect of MG624, StN-4 and StN-8 on cell cycle phases distribution in U87MG cells.

A) Representative histogram plots generated after FACS analysis of U87MG cells treated for 72 hours with 4 μM MG624, 2 μM StN-4 or 0.25 μM StN-8 and stained with propidium iodide (PI).

B) The percentage of U87MG cells in each phase of the cell cycle (G_1/G_0, S or G_2/M) has been quantified after 72 hours of treatment with the compounds at the indicated concentrations.The values expressed are the mean ± SEM. **p < 0.01 , **p < 0.001 , ****p < 0.0001 increase (G_1/G_0) or decrease (S and G_2/M) of each phase over untreated cells. The data were analysed by means of a one-way ANOVA followed by a Bonferroni's post hoc test.

Figure 7

MG624 and StN-4 treatment induced apoptosis in U87MG cells.

A) Representative dot plots were generated by FACS analysis of U87MG cells exposed to the indicated concentrations of MG624, StN-4, and StN-8 for 72 hours and stained with Annexin V-FITC and propidium iodide (PI).

B) MG624 and StN-4 at the indicated concentrations increase apoptotic rate of U87MG cells after 72 hours of exposure, as revealed by Annexin V-FITC and PI staining. The values expressed are the mean ± SEM *p < 0.05: increase over untreated cells. The data were analysed by means of one-way ANOVA followed by a Bonferroni's post hoc test.

Figure 8

MG624, StN-4 and StN-8 decrease the activation of AKT signalling pathway

U87MG cells were exposed for 72 hours to the indicated concentrations of the compounds and the quantifications of the Western blots are expressed as the decrease in the pAKT/AKT ratio (with the untreated cells taken as 1).

A) The presence of the α7/α9 nicotinic antagonist αBgtx did not influence the compounds-induced decrease of Ser473-AKT phosphorylation. The graph shows the mean values ± SEM of each group obtained from the indicated number of experiments.

A representative blot at the corresponding times is shown below each graph. *p < 0.05, **p < 0.01, ****p < 0.0001: decrease over untreated cells. The data were analysed by means of a Kruskall-Wallis test followed by a Dunn's post hoc test.

9. References

[1] A. Jemal, F. Bray, M.M. Center, J. Ferlay, E. Ward, D. Forman, Global cancer statistics, CA Cancer J Clin 61(2) (2011) 69-90.

[2] M. Dobes, V.G. Khurana, B. Shadbolt, S. Jain, S.F. Smith, R. Smee, M. Dexter, R. Cook, Increasing incidence of glioblastoma multiforme and meningioma, and decreasing incidence of Schwannoma (2000-2008): Findings of a multicenter Australian study, Surg Neurol Int 2 (2011) 176.

[3] P. Zhu, X.L. Du, G. Lu, J.J. Zhu, Survival benefit of glioblastoma patients after FDA approval of temozolomide concomitant with radiation and bevacizumab: A population-based study, Oncotarget 8(27) (2017) 44015-44031.

[4] Q.T. Ostrom, H. Gittleman, J. Fulop, M. Liu, R. Blanda, C. Kromer, Y. Wolinsky, C. Kruchko, J.S. Barnholtz-Sloan, CBTRUS Statistical Report: Primary Brain and Central Nervous System Tumors Diagnosed in the United States in 2008-2012, Neuro Oncol 17 Suppl 4 (2015) iv1-iv62.

[5] O.G. Taylor, J.S. Brzozowski, K.A. Skelding, Glioblastoma Multiforme: An Overview of Emerging Therapeutic Targets, Front Oncol 9 (2019) 963.

[6] G.P. Dunn, M.L. Rinne, J. Wykosky, G. Genovese, S.N. Quayle, I.F. Dunn, P.K. Agarwalla, M.G. Chheda, B. Campos, A. Wang, C. Brennan, K.L. Ligon, F. Furnari, W.K. Cavenee, R.A. Depinho, L. Chin, W.C. Hahn, Emerging insights into the molecular and cellular basis of glioblastoma, Genes Dev 26(8) (2012) 756-84.

[7] S. Alcantara Llaguno, D. Sun, A.M. Pedraza, E. Vera, Z. Wang, D.K. Burns, L.F. Parada, Cell-of-origin susceptibility to glioblastoma formation declines with neural lineage restriction, Nat Neurosci 22(4) (2019) 545-555.

[8] R. Yamada, I. Nakano, Glioma stem cells: their role in chemoresistance, World Neurosurg 77(2) (2012) 237-40.

[9] K. Desai, A. Hubben, M. Ahluwalia, The Role of Checkpoint Inhibitors in Glioblastoma, Target Oncol 14(4) (2019) 375-394.

[10] A.A. Khalil, M.J. Jameson, W.C. Broaddus, P.S. Lin, T.D. Chung, Nicotine enhances proliferation, migration, and radioresistance of human malignant glioma cells through EGFR activation, Brain Tumor Pathol 30(2) (2013) 73-83.

[11] R. Spina, D.M. Voss, L. Asnaghi, A. Sloan, E.E. Bar, Atracurium Besylate and other neuromuscular blocking agents promote astroglial differentiation and deplete glioblastoma stem cells, Oncotarget 7(1) (2016) 459-72.

[12] E.G. Thompson, H. Sontheimer, Acetylcholine Receptor Activation as a Modulator of Glioblastoma Invasion, Cells 8(10) (2019).

[13] S. Pucci, F. Fasoli, M. Moretti, R. Benfante, S. Di Lascio, P. Viani, A. Daga, T.J. Gordon, M. McIntosh, M. Zoli, F. Clementi, C. Gotti, Choline and nicotine increase glioblastoma cell proliferation by binding and activating alpha7- and alpha9- containing nicotinic receptors, Pharmacol Res 163 (2021) 105336.

[14] V. Mucchietto, F. Fasoli, S. Pucci, M. Moretti, R. Benfante, A. Maroli, S. Di Lascio, C. Bolchi, M. Pallavicini, C. Dowell, M. McIntosh, F. Clementi, C. Gotti, alpha9- and alpha7-containing receptors mediate the pro-proliferative effects of nicotine in the A549 adenocarcinoma cell line, Br J Pharmacol 175(11) (2018) 1957-1972.

[15] C. Gotti, B. Balestra, M. Moretti, G.E. Rovati, L. Maggi, G. Rossoni, F. Berti, L. Villa, M. Pallavicini, F. Clementi, 4-Oxystilbene compounds are selective ligands for neuronal nicotinic alphaBungarotoxin receptors, Br J Pharmacol 124(6) (1998) 1197-206.

[16] L. Maggi, E. Palma, F. Eusebi, M. Moretti, B. Balestra, F. Clementi, C. Gotti, Selective effects of a 4-oxystilbene derivative on wild and mutant neuronal chick alpha7 nicotinic receptor, Br J Pharmacol 126(1) (1999) 285-95.

[17] F. Bavo, S. Pucci, F. Fasoli, C. Lammi, M. Moretti, V. Mucchietto, D. Lattuada, P. Viani, C. De Palma, R. Budriesi, I. Corradini, C. Dowell, J.M. McIntosh, F. Clementi, C. Bolchi, C. Gotti, M. Pallavicini, Potent Antiglioblastoma Agents by Hybridizing the Onium-Alkyloxy-Stilbene Based Structures of an alpha7-nAChR, alpha9-nAChR Antagonist and of a Pro-Oxidant Mitocan, J Med Chem 61(23) (2018) 10531-10544.

[18] K.C. Brown, J.K. Lau, A.M. Dom, T.R. Witte, H. Luo, C.M. Crabtree, Y.H. Shah, B.S. Shiflett, A.J. Marcelo, N.A. Proper, W.E. Hardman, R.D. Egleton, Y.C. Chen, E.I. Mangiarua, P. Dasgupta, MG624, an alpha7-nAChR antagonist, inhibits angiogenesis via the Egr-1/FGF2 pathway, Angiogenesis 15(1) (2012) 99-114.

[19] E. Mirhadi, B.D. Roufogalis, M. Banach, M. Barati, A. Sahebkar, Resveratrol: Mechanistic and therapeutic perspectives in pulmonary arterial hypertension, Pharmacol Res 163 (2021) 105287.

[20] L. Biasutto, I. Szabo, M. Zoratti, Mitochondrial effects of plant-made compounds, Antioxid Redox Signal 15(12) (2011) 3039-59.

[21] L. Biasutto, A. Mattarei, E. Marotta, A. Bradaschia, N. Sassi, S. Garbisa, M. Zoratti, C. Paradisi, Development of mitochondria-targeted derivatives of resveratrol, Bioorg Med Chem Lett 18(20) (2008) 5594-7.

[22] N. Sassi, A. Mattarei, M. Azzolini, P. Bernardi, I. Szabo, C. Paradisi, M. Zoratti, L. Biasutto, Mitochondria-targeted resveratrol derivatives act as cytotoxic pro-oxidants, Curr Pharm Des 20(2) (2014) 172-9.

[23] B. Banelli, E. Carra, F. Barbieri, R. Wurth, F. Parodi, A. Pattarozzi, R. Carosio, A. Forlani, G. Allemanni, D. Marubbi, T. Florio, A. Daga, M. Romani, The histone demethylase KDM5A is a key factor for the resistance to temozolomide in glioblastoma, Cell Cycle 14(21) (2015) 3418-29.

[24] R.L. Papke, J.M. Lindstrom, Nicotinic acetylcholine receptors: Conventional and unconventional ligands and signaling, Neuropharmacology 168 (2020) 108021.

[25] M. Zoli, F. Pistillo, C. Gotti, Diversity of native nicotinic receptor subtypes in mammalian brain, Neuropharmacology 96(Pt B) (2015) 302-11.

[26] A.B. Elgoyhen, D.S. Johnson, J. Boulter, D.E. Vetter, S. Heinemann, Alpha 9: an acetylcholine receptor with novel pharmacological properties expressed in rat cochlear hair cells, Cell 79(4) (1994) 705-15.

[27] B. De Filippis, A. Ammazzalorso, M. Fantacuzzi, L. Giampietro, C. Maccallini, R. Amoroso, Anticancer Activity of Stilbene-Based Derivatives, ChemMedChem 12(8) (2017) 558-570.

[28] R.J. Chen, H.C. Kuo, L.H. Cheng, Y.H. Lee, W.T. Chang, B.J. Wang, Y.J. Wang, H.C. Cheng, Apoptotic and Nonapoptotic Activities of Pterostilbene against Cancer, Int J Mol Sci 19(1) (2018).

[29] J.S. Brown, U. Banerji, Maximising the potential of AKT inhibitors as anti-cancer treatments, Pharmacol Ther 172 (2017) 101-115.

[30] B.J. Morley, P. Whiteaker, A.B. Elgoyhen, Commentary: Nicotinic Acetylcholine Receptor alpha9 and alpha10 Subunits Are Expressed in the Brain of Mice, Front Cell Neurosci 12 (2018) 104.

[31] S. Fucile, M. Renzi, P. Lax, F. Eusebi, Fractional Ca(2+) current through human neuronal alpha7 nicotinic acetylcholine receptors, Cell Calcium 34(2) (2003) 205-9.

[32] S. Fucile, A. Sucapane, F. Eusebi, Ca2+ permeability through rat cloned alpha9-containing nicotinic acetylcholine receptors, Cell Calcium 39(4) (2006) 349-55.

[33] M. Lund-Johansen, R. Bjerkvig, P.A. Humphrey, S.H. Bigner, D.D. Bigner, O.D. Laerum, Effect of epidermal growth factor on glioma cell growth, migration, and invasion in vitro, Cancer Res 50(18) (1990) 6039-44.

[34] V. Venkataramani, D.I. Tanev, C. Strahle, A. Studier-Fischer, L. Fankhauser, T. Kessler, C. Korber, M. Kardorff, M. Ratliff, R. Xie, H. Horstmann, M. Messer, S.P. Paik, J. Knabbe, F. Sahm, F.T. Kurz, A.A. Acikgoz, F. Herrmannsdorfer, A. Agarwal, D.E. Bergles, A. Chalmers, H. Miletic, S. Turcan, C. Mawrin, D. Hanggi, H.K. Liu, W. Wick, F. Winkler, T. Kuner, Glutamatergic synaptic input to glioma cells drives brain tumour progression, Nature 573(7775) (2019) 532-538.

[35] J. Corradi, C. Bouzat, Understanding the Bases of Function and Modulation of alpha7 Nicotinic Receptors: Implications for Drug Discovery, Mol Pharmacol 90(3) (2016) 288-99.

[36] G. Sharma, S. Vijayaraghavan, Nicotinic cholinergic signaling in hippocampal astrocytes involves calcium-induced calcium release from intracellular stores, Proc Natl Acad Sci U S A 98(7) (2001) 4148-53.

[37] D.A. Fruman, C. Rommel, PI3K and cancer: lessons, challenges and opportunities, Nat Rev Drug Discov 13(2) (2014) 140-56.

[38] M.D. Altintop, B. Sever, G. Akalin Ciftci, A. Ozdemir, Design, Synthesis, and Evaluation of a New Series of Thiazole-Based Anticancer Agents as Potent Akt Inhibitors, Molecules 23(6) (2018).

[39] B. Haas, V. Klinger, C. Keksel, V. Bonigut, D. Kiefer, J. Caspers, J. Walther, M. Wos-Maganga, S. Weickhardt, G. Rohn, M. Timmer, R. Frotschl, N. Eckstein, Inhibition of the PI3K but not the MEK/ERK pathway sensitizes human glioma cells to alkylating drugs, Cancer Cell Int 18 (2018) 69.

[40] Y. Cheng, Y. Zhang, L. Zhang, X. Ren, K.J. Huber-Keener, X. Liu, L. Zhou, J. Liao, H. Keihack, L. Yan, E. Rubin, J.M. Yang, MK-2206, a novel allosteric inhibitor of Akt, synergizes with gefitinib against malignant glioma via modulating both autophagy and apoptosis, Mol Cancer Ther 11(1) (2012) 154-64.

[41] P.E. Porporato, N. Filigheddu, J.M.B. Pedro, G. Kroemer, L. Galluzzi, Mitochondrial metabolism and cancer, Cell Res 28(3) (2018) 265-280.

[42] Q. Cui, S. Wen, P. Huang, Targeting cancer cell mitochondria as a therapeutic approach: recent updates, Future Med Chem 9(9) (2017) 929-949.

[43] E. Vlashi, C. Lagadec, L. Vergnes, T. Matsutani, K. Masui, M. Poulou, R. Popescu, L. Della Donna, P. Evers, C. Dekmezian, K. Reue, H. Christofk, P.S. Mischel, F. Pajonk, Metabolic state of glioma stem cells and nontumorigenic cells, Proc Natl Acad Sci U S A 108(38) (2011) 16062-7.

[44] G. Gergalova, O. Lykhmus, O. Kalashnyk, L. Koval, V. Chernyshov, E. Kryukova, V. Tsetlin, S. Komisarenko, M. Skok, Mitochondria express alpha7 nicotinic acetylcholine receptors to regulate Ca2+ accumulation and cytochrome c release: study on isolated mitochondria, PLoS One 7(2) (2012) e31361.

[45] O.M. Kalashnyk, G.L. Gergalova, S.V. Komisarenko, M.V. Skok, Intracellular localization of nicotinic acetylcholine receptors in human cell lines, Life Sci 91(21-22) (2012) 1033-7.

[46] K. Uspenska, O. Lykhmus, M. Obolenskaya, S. Pons, U. Maskos, S. Komisarenko, M. Skok, Mitochondrial Nicotinic Acetylcholine Receptors Support Liver Cells Viability After Partial Hepatectomy, Front Pharmacol 9 (2018) 626.

List of chemical compounds

Acetylcholine
αBungarotoxin
H_2DCFDA
MG624
Nicotine
PNU120596
StN-4
StN-8
tetramethylrhodamine, methyl ester
tert-butyl hydroperoxide

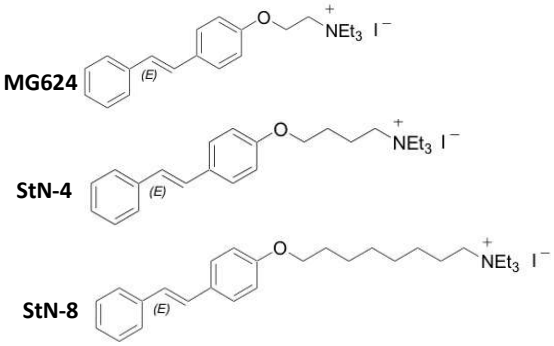

Fig. 1

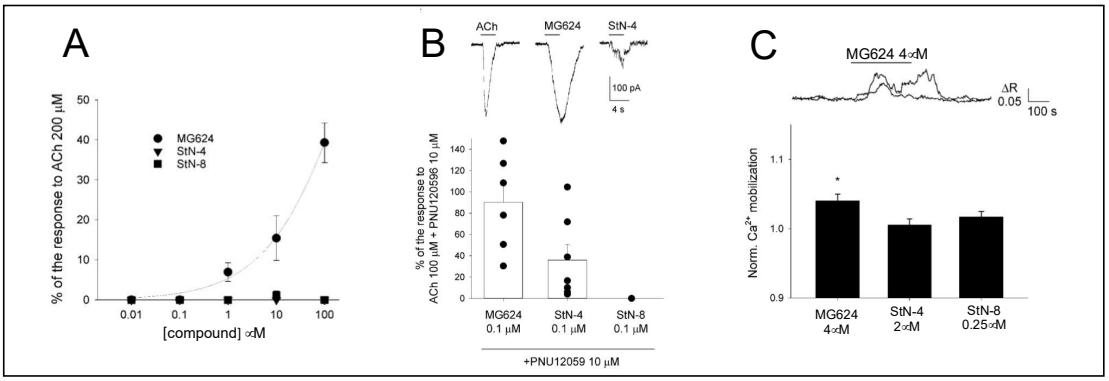

Fig. 2

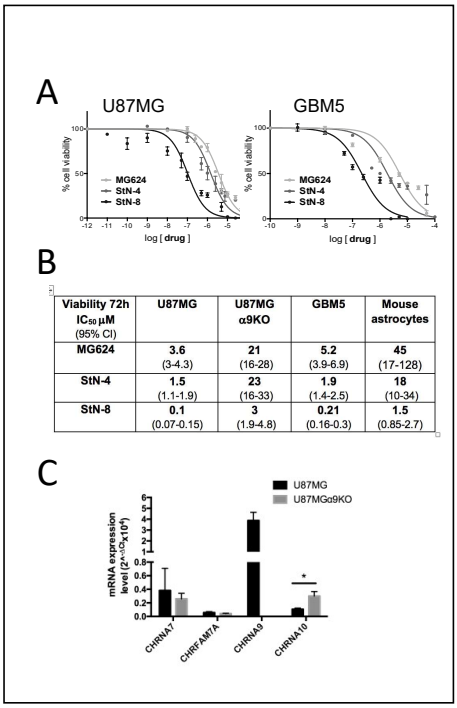

Viability 72h IC_{50} µM (95% CI)	U87MG	U87MG α9KO	GBM5	Mouse astrocytes
MG624	3.6 (3-4.3)	21 (16-28)	5.2 (3.9-6.9)	45 (17-128)
StN-4	1.5 (1.1-1.9)	23 (16-33)	1.9 (1.4-2.5)	18 (10-34)
StN-8	0.1 (0.07-0.15)	3 (1.9-4.8)	0.21 (0.16-0.3)	1.5 (0.85-2.7)

Fig. 3

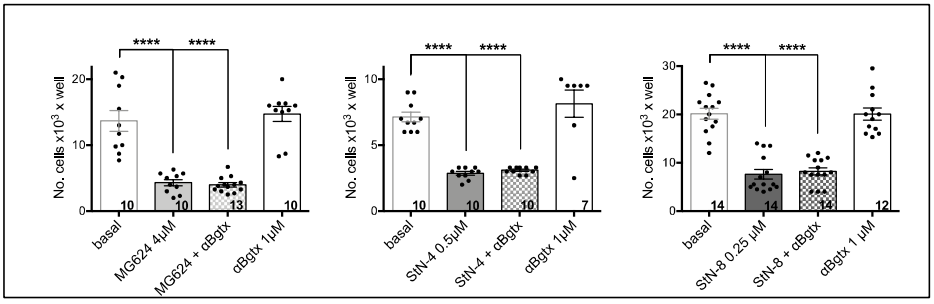
No. cells x10^3 x well
basal
MG624 4µM
MG624 + dBgtx
dBgtx 1µM
StN-4 0.5µM
StN-4 + dBgtx
StN-8 0.25 µM
StN-8 + dBgtx
dBgtx 1 µM

Fig. 4

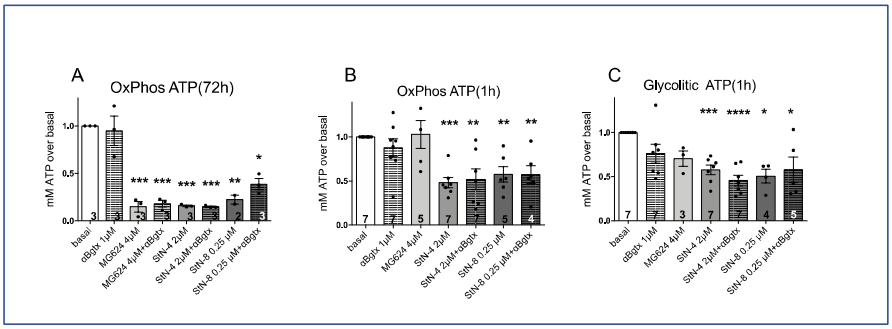
A
OxPhos ATP(72h)
B
OxPhos ATP(1h)
C
Glycolitic ATP(1h)
mM ATP over basal

Fig. 5

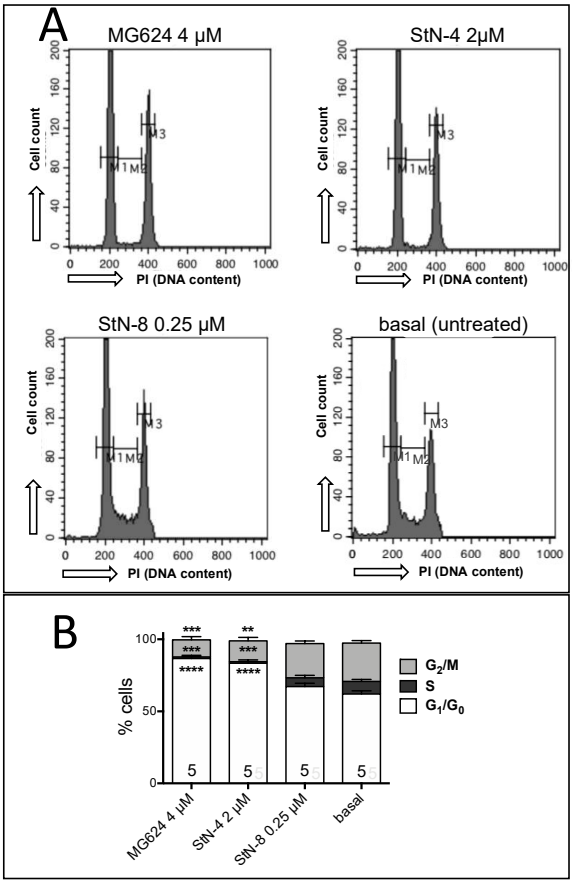
A
MG624 4 µM
StN-4 2µM
StN-8 0.25 µM
basal (untreated)
Cell count
PI (DNA content)
M1
M2
M3
B
% cells
G2/M
S
G1/G0
MG624 4 µM
StN-4 2 µM
StN-8 0.25 µM
basal

Fig. 6

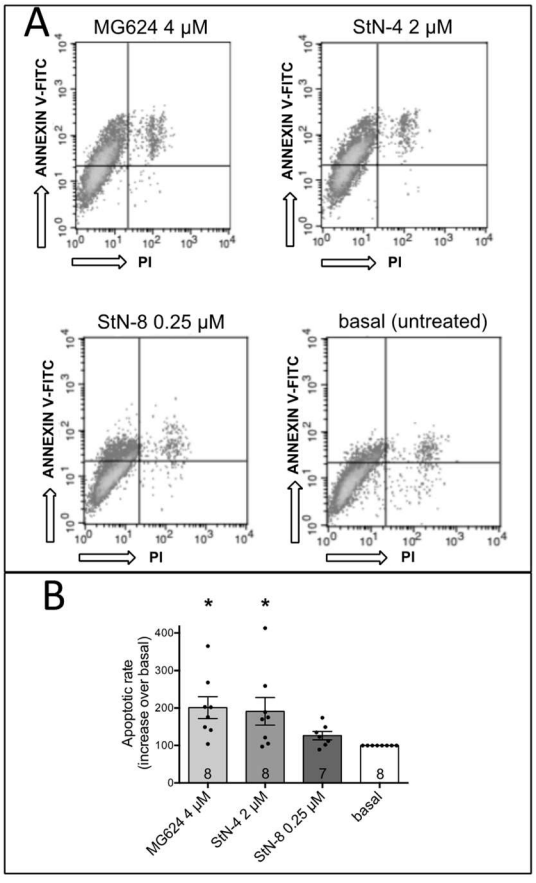
A
MG624 4 µM
StN-4 2 µM
StN-8 0.25 µM
basal (untreated)
ANNEXIN V-FITC
PI
B
Apoptotic rate
(increase over basal)
MG624 4 µM
StN-4 2 µM
StN-8 0.25 µM
basal

Fig. 7

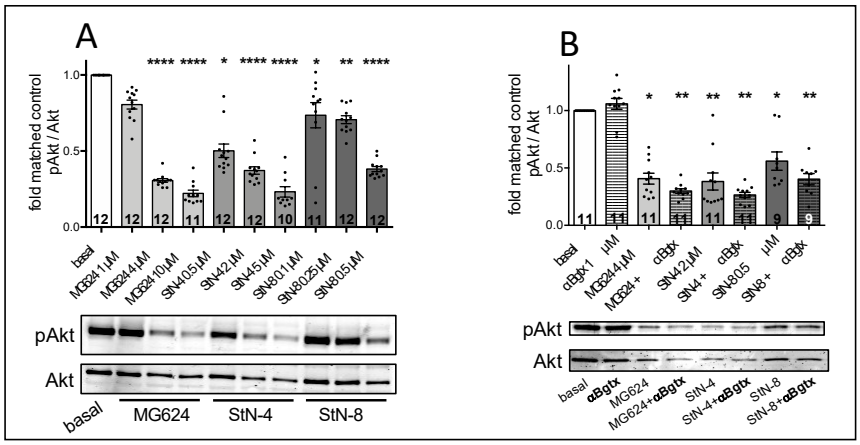

Fig. 8

Supplementary material

Figure S1

Effect of MG624, StN-4 and StN-8 treatment on total ROS production in U87MG cells

A) Representative histogram plots generated after FACS analysis of U87MG cells treated for 4 hours with 4 μM MG624, 2 μM StN-4, 0.25 μM StN-8 or the positive control 50 μM TBHP and stained with H_2DCFDA. We assumed positive cells for the staining as those included within the M1 gate, which excludes the untreated (negative) cells.

B) The percentage of stained U87MG cells has been quantified after 4 hours of treatment with the compounds at the indicated concentrations and normalized over the cells treated with the positive control TBHP:

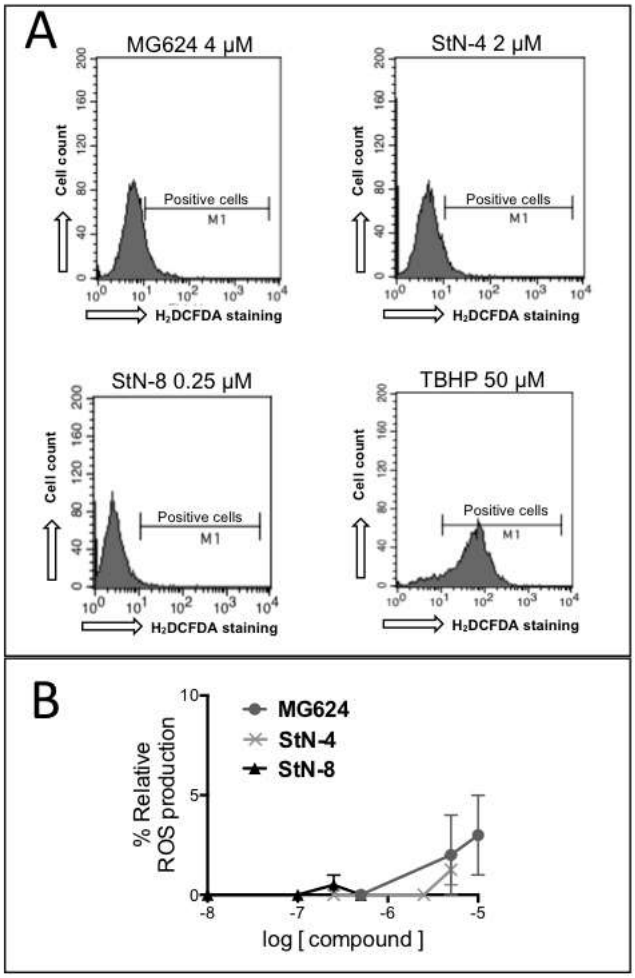

Fig. S1

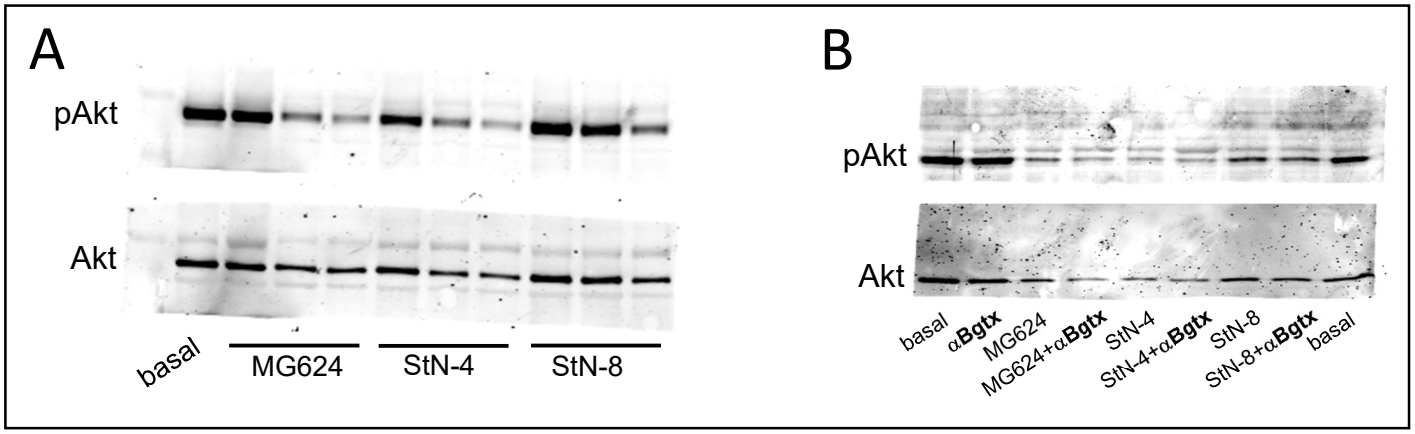

Uncropped WB fig.8